Energy Conversion and Management 89 (2015) 719–726

Contents lists available at ScienceDirect

Energy Conversion and Management

journal homepage: www.elsevier.com/locate/enconman

Grid-friendly wind power systems based on the synchronverter technology ☆

Qing-Chang Zhong [a,c,*], Zhenyu Ma [b], Wen-Long Ming [a], George C. Konstantopoulos [a]

[a] Dept. of Automatic Control and Systems Engineering, The University of Sheffield, Sheffield S1 3JD, UK
[b] CSR Zhuzhou Electric Locomotive Co., LTD, Shidai Road, Hunan Province, ZhuZhou 412001, China
[c] Department of Power Distribution, China Electric Power Research Institute, Beijing 100192, China

ARTICLE INFO

Article history:
Received 4 May 2014
Accepted 11 October 2014
Available online 6 November 2014

Keywords:
Synchronverter
Inverters that mimic synchronous generators
Back-to-back converters
Wind turbine
Maximum power point tracking (MPPT)
Grid faults

ABSTRACT

Back-to-back PWM converters are becoming a realistic alternative to conventional converters in high-power wind power applications. In this paper, a control strategy based on the synchronverter technology is proposed for back-to-back PWM converters. Both converters are run as synchronverters, which are mathematically equivalent to the conventional synchronous generators. The rotor-side converter is responsible for maintaining the DC link voltage and the grid-side converter is responsible for the maximum power point tracking (MPPT). As the two converters are operated using the synchronverter technology, the formed wind power system becomes more friendly to the grid. Extensive real-time digital simulation results are presented to verify the effectiveness of the proposed method under normal operation and grid-fault scenarios.

1. Introduction

During the last decade, more and more attention has been paid towards utilising renewable energy sources to tackle the energy crisis we are facing. Wind power has been regarded as one of the main renewable power sources to replace/complement fossil fuels. Wind energy offers many advantages such as no environmental pollution, relatively low capital cost involved and a short gestation period. Therefore, many countries have set strategic plans to develop technologies for utilising wind power and a lot of researchers have shifted into this area.

Wind generation systems can be divided into variable-speed and fixed-speed generation systems. Variable-speed systems are more attractive than fixed-speed systems due to the improved wind energy production and its reduction of flicker problems. Nowadays, the most commonly-used topologies for variable-speed wind turbines include doubly-fed induction generators with wounded rotors, induction generators with squirrel cage rotors and synchronous generators with permanent magnets (PMSG) [1–4]. In these three cases, one of the most popular grid connection topologies is to adopt back-to-back voltage source inverters to interface with the grid [5–9] on order to provide unity power factor and low harmonic distortion of the current, and to operate the wind farm for provision of ancillary services such as low voltage ride through capability. The synchronous generator is connected to the grid through a full-scale back-to-back PWM converter and the conversion stage consists of a rotor-side converter and a grid-side converter, as shown in Fig. 1. Although this topology is widely used because it simplifies the control design, it has a substantial influence on power quality, because non-sinusoidal currents delivered to the grid can introduce an additional non-sinusoidal voltage drop across the line impedance. This increases the grid voltage distortion, which affects other loads and/or generators.

Many different control strategies have been developed for back-to-back PWM converters in wind power applications. Normally, the maximum power extraction from the wind is achieved by controlling the rotor-side converter and the DC link voltage is controlled by the grid-side converter [10–17]. In this case, the DC link voltage is increased due to the continuous operation of the wind turbine and the generator when grid faults occur. The grid-side converter may be out of control when grid voltage sags occur because voltage sags reduce generator torque [18], which accelerates the rotor and causes mechanical instability, unless normal

☆ A preliminary version of this article was presented at the 8th IFAC Symposium on Power Plants and Power Systems Control (PP&PSC), Toulouse, France, September 2012.

* Corresponding author at: Dept. of Automatic Control and Systems Engineering, The University of Sheffield, Sheffield S1 3JD, UK.
E-mail addresses: zhongqc@ieee.org (Q.-C. Zhong), ma_zhenyu@hotmail.com (Z. Ma), w.ming@sheffield.ac.uk (W.-L. Ming), g.konstantopoulos@sheffield.ac.uk (G.C. Konstantopoulos).

http://dx.doi.org/10.1016/j.enconman.2014.10.027
0196-8904/

voltage levels are quickly restored. As a fail-safe mechanism against equipment damage, wind turbines are designed to automatically disconnect themselves from the utility grid under these extreme conditions [19,20]. Therefore, in some other strategies, the rotor-side converter controls the DC link voltage and the grid-side converter controls the power of the wind turbine fed to the grid [21–23]. In both cases, the control strategies are mainly based on the vector control approach in the d-q reference frame to control the direct component and the quadrature component, respectively [24]. Due to the decoupling terms used for achieving the desired field-orientation, vector control techniques become sensitive to parameters variation and mismatch.

In this paper, an original control strategy based on the synchronverter technology, which is to operate a converter to mimic a synchronous machine [25], is proposed for back-to-back converters in wind power applications. The rotor-side converter is run as a synchronous motor, since it receives power from the PMSG at the AC side and injects it to the DC link. The main tasks of the rotor-side converter are to regulate the DC link voltage to the desired level and to achieve unity power factor operation at the AC side. Opposed to the existing vector control techniques, the synchronverter technology is completely independent from the parameters of the PMSG, providing significant advantages to the system performance. The knowledge of the stator inductance or the rotor time constant of the PMSG is not required for the synchronverter implementation. In the same frame, the grid-side converter is run as a synchronous generator, since it injects real and reactive power to the grid. The main tasks of the grid-side converter are to achieve maximum power point tracking (MPPT), i.e. maximum power extraction from the wind, and also regulate the reactive power. As a result, the whole system behaves as a generator–motor–generator system, which leads to a complete, compact and effective system operation. Compared to the vector control, the synchronverter technology makes wind turbine systems more friendly to the power grid, which is dominated by synchronous generators.

The rest of the paper is organised as follows. The synchronverter technology is outlined in Section 2. The control strategy for rotor-side converter is discussed in Section 3 and the control strategy for grid-side converter is discussed in Section 4. The real-time simulation results for the complete wind power system are provided in Section 5.

2. Overview of the synchronverter technology

A synchronverter is an inverter (converter) that mimics a synchronous generator (machine). The core of the controller is the mathematical model of a synchronous generator, which is then wrapped with some functions to regulate the real power and reactive power, the voltage and the frequency. In this paper, the controllers wrapped around the model will be developed according to the applications of wind power systems. Hence, only the mathematical model of synchronous machines is outlined, as this is the core for the controllers of the two converters.

Assume that the three identical stator windings of a synchronous generator are distributed in slots around the periphery of the uniform air gap. The stator windings can be regarded as concentrated coils having self-inductance L, mutual inductance $-M$ (with $M > 0$, the negative sign is due to the $\frac{2\pi}{3}$ phase angle) and resistance R_s (see Fig. 2).

Denote the flux vector and the current vector as

$$\Phi = \begin{bmatrix} \Phi_a \\ \Phi_b \\ \Phi_c \end{bmatrix}, \quad i = \begin{bmatrix} i_a \\ i_b \\ i_c \end{bmatrix},$$

respectively, and the vectors

$$\widetilde{\cos}\theta = \begin{bmatrix} \cos\theta \\ \cos\left(\theta - \frac{2\pi}{3}\right) \\ \cos\left(\theta - \frac{4\pi}{3}\right) \end{bmatrix}, \quad \widetilde{\sin}\theta = \begin{bmatrix} \sin\theta \\ \sin\left(\theta - \frac{2\pi}{3}\right) \\ \sin\left(\theta - \frac{4\pi}{3}\right) \end{bmatrix},$$

where θ is the rotor angle with respect to the phase a winding. Then the phase terminal voltages $v = [\, v_a \quad v_b \quad v_c \,]^T$ of a generator can be written as

$$v = e - R_s i - L_s \frac{di}{dt}, \tag{1}$$

where $L_s = L + M$ and $e = [\, e_a \quad e_b \quad e_c \,]^T$ is the back emf due to the rotor movement given by

$$e = M_f i_f \dot{\theta} \widetilde{\sin}\theta - M_f \frac{di_f}{dt} \widetilde{\cos}\theta. \tag{2}$$

The mechanical part of the generator is governed by

$$\ddot{\theta} = \frac{1}{J}(T_m - T_e - D_p \dot{\theta}), \tag{3}$$

where J is the moment of inertia of all the parts rotating with the rotor; D_p is a damping factor; T_m is the mechanical torque and T_e is the electromagnetic torque

$$T_e = M_f i_f \left\langle i, \widetilde{\sin}\theta \right\rangle, \tag{4}$$

where $\langle \cdot, \cdot \rangle$ denotes the conventional inner product in $\mathbb{R}^3$.

The real power and reactive power are, respectively,

$$P = \dot{\theta} M_f i_f \langle i, \widetilde{\sin}\theta \rangle,$$
$$Q = -\dot{\theta} M_f i_f \langle i, \widetilde{\cos}\theta \rangle. \tag{5}$$

The model can be described from the block diagram shown in Fig. 3.

3. Control of the rotor-side converter

As mentioned before, the main task of the rotor-side converter is to maintain a constant DC-link voltage. Hence, the converter is run as a PWM rectifier. Here, this is done via operating the PWM rectifier to mimic a synchronous motor.

Denote the output voltage and current of the wind-turbine generator as $v_r = [\, v_{ra} \quad v_{rb} \quad v_{rc} \,]^T$ and $i_r = [\, i_{ra} \quad i_{rb} \quad i_{rc} \,]^T$, respectively. The proposed control strategy is shown in Fig. 4, which includes the model of a synchronous motor as the core of the control strategy. The model of a synchronous motor coincides with the model of a generator discussed above, apart from the fact that the stator current is defined in the opposite direction. Therefore, Eqs. (1) and (3) should be modified accordingly as

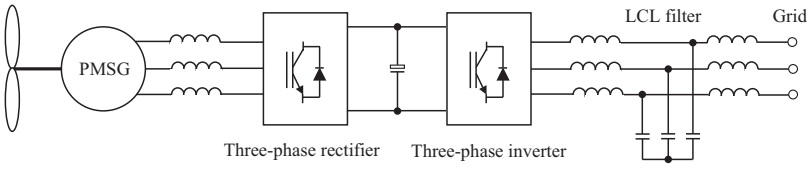

Fig. 1. Connection of wind power generation system to grid through back-to-back converters.

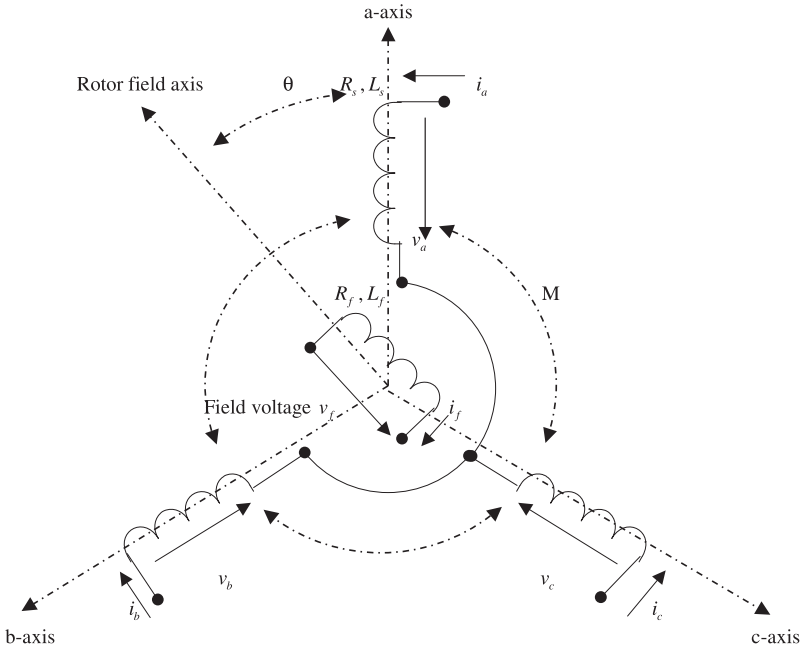

Fig. 2. Structure of an idealised three-phase round-rotor synchronous machine.

$$v_r = e_m + R_s i_r + L_s \frac{di_r}{dt},$$

and

$$\ddot{\theta}_m = \frac{1}{J_m}(T_{me} - T_{mm} - D_{mp}\dot{\theta}_m),$$

where the mechanical torque T_{mm} is the load torque of the motor. Here, the torque T_{mm} is generated by the PI controller that regulates the DC-link voltage.

In order for the rotor-side converter, i.e., the virtual synchronous motor, to work properly, the frequency $\dot{\theta}_m$ inside the rectifier should be the same or very close to the frequency $\dot{\theta}_r$ of v_r and the terminal voltage should be synchronised with the voltage v_r. Before the rectifier is connected to v_r, its phase θ_m should be kept the same as that of v_r in order to minimise the settling time following the connection. The traditional phase-locked loop (PLL) in the dq frame is not fast enough for this purpose [26]. In this paper, the sinusoid-tracking algorithm (STA) [27] is adopted to quickly provide the frequency and the phase information of the voltage signal.

The control strategy involves two channels: one channel to regulate the real power and another to regulate the reactive power. The real power channel, shown in Fig. 4, has three cascaded control loops. The inner loop is the frequency regulation loop (with the feedback gain D_{mp}), the middle loop is a torque loop (with the feedback coming from the current i_r via the electromagnetic torque T_{me}) and the outer loop is the DC-link voltage loop (with the feedback coming from the DC voltage V_{dc}). The first two loops are part of the model of a virtual synchronous motor.

When the rotor-side converter is connected to v_r, its virtual frequency should track the frequency of v_r. This can be done via feeding the difference between the frequency $\dot{\theta}_r$ obtained from the STA and the rectifier frequency $\dot{\theta}_m$ to the D_{mp} block, as done in the original synchronverter [25]. In this case, the constant D_{mp} represents the (imaginary) mechanical friction coefficient of the virtual motor. The frequency droop coefficient is defined as $D_{mp} = -\frac{\Delta T}{\Delta \dot{\theta}_m}$, where ΔT denotes the amount of change in the torque that leads to the change $\Delta\dot{\theta}_m$ in the frequency.

The reactive power Q_m of the rotor-side converter can be controlled to track the reference Q_{ref}. The tracking error between the reference value Q_{ref} and reactive power Q_m is fed into an integrator with a gain $-\frac{1}{K}$ to regulate the field excitation $M_f i_f$ so that the voltage e_m is changed accordingly. In order to obtain the unity power factor, Q_{ref} can be set equal to 0.

4. Control of the grid-side converter

The control objective for the grid-side converter is to send the maximum power generated from wind to the grid. Normally, variable-speed wind generation systems are more attractive than fixed-speed systems due to the high efficiency. However, this does not necessarily mean that the actual efficiency is always high in variable-speed generator systems. It depends on the control algorithm used to extract the output power from the wind turbine. A technique based on wind power curves will be designed to extract the maximum power from the wind turbine under all working conditions. In variable-speed generation systems, the wind turbine can be operated at its maximum power operating point for various

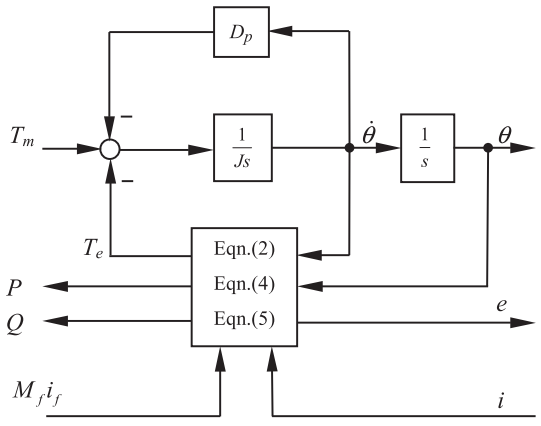

Fig. 3. The model of a synchronous machine.

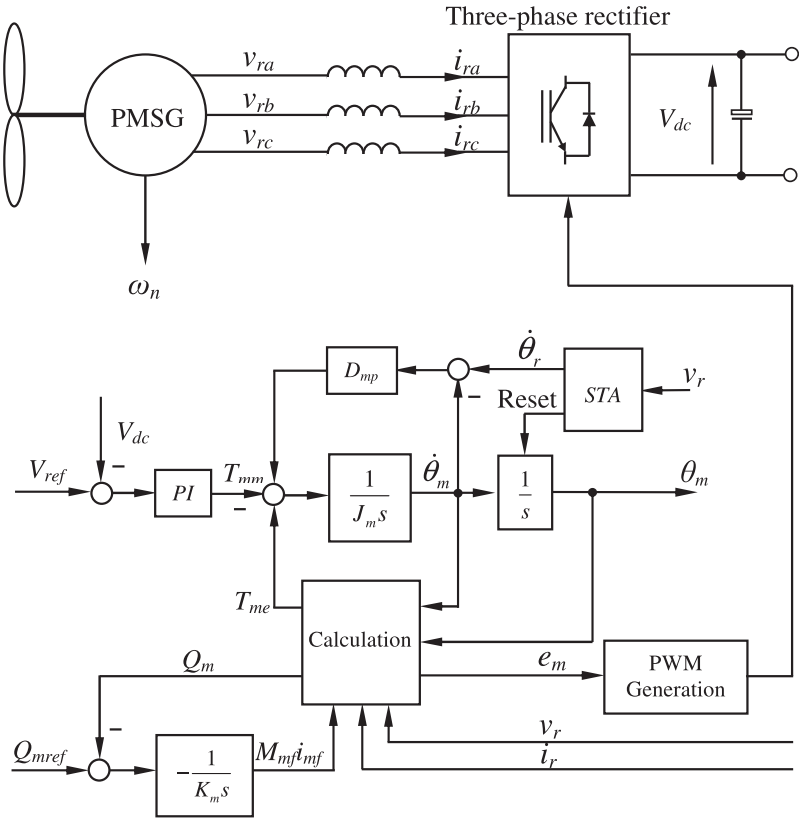

Fig. 4. Control structure for the rotor-side converter.

wind speeds by maintaining the tip speed ratio to the value that maximises its aerodynamic efficiency. In order to achieve this ratio, the permanent magnet synchronous generator load line should be matched very closely to the maximum power line of the wind turbine.

In a variable-speed wind turbine, the power P_w that can be obtained from the wind is a cubic function of the wind speed v_w, i.e,

$$P_w = \frac{1}{2}\rho\pi R^2 v_w^3 C_p, \tag{6}$$

where ρ is the air density, R is the turbine radius and $C_p = f(\lambda, \beta)$ is the power coefficient that depends on the tip speed ratio λ of the wind turbine and the angle of blades β. The tip speed ratio is defined as

$$\lambda = \frac{\omega_n R}{v_w},$$

where ω_n is the rotor speed of the turbine. Consequently, for different wind speeds, the optimal values of the tip speed and the pitch angle need to be followed in order to achieve the maximum C_p and therefore the maximum power output. The maximum power of the wind turbine can be calculated as

$$P_m = \frac{1}{2}\rho\pi R^2 C_{pm}\left(\frac{R\omega_n}{\lambda_{opt}}\right)^3 = K_{opt}\omega_n^3,$$

where $K_{opt} = \frac{1}{2}\rho\pi C_{pm}\left(\frac{R^5}{\lambda_{opt}^3}\right)$. Taking the losses into account, the grid power reference can be chosen slightly smaller than P_m. In this paper, this is chosen as

$$P_{ref} = 0.95 K_{opt}\omega_n^3 \tag{7}$$

The coefficient, 0.95, is the estimated value after considering losses, which may be changed for different systems. Taking into account the converter and the PMSG ratings, the coefficient can be estimated by considering a wide range of wind speeds to cover all possible scenarios. This reference can be passed to the synchronverter so that the right amount of power is fed into the grid. The proposed control strategy for the grid-side converter is shown in Fig. 5, where the inductor current, the capacitor voltage and the grid voltage are denoted as $i = [\,i_a \quad i_b \quad i_c\,]^T$, $v = [\,v_a \quad v_b \quad v_c\,]^T$ and $v_g = [\,v_{ga} \quad v_{gb} \quad v_{gc}\,]^T$, respectively. This is very similar to the controller for the synchronverter [25], with the real power reference set from (7). Because of the inherent capability of the synchronverter, this strategy is able to feed the real power to the grid while regulating the reactive power.

5. Real-time simulation results

Real-time simulations were carried out to verify the control strategy described above using an OPAL RT real-time digital simulation system. The back-to-back converter was implemented using the universal bridge with IGBTs as switches, and the switching frequency was set to 5 kHz. The other parameters of the system used in the simulations are given in Table 1.

The wind turbine extracts power from wind and then converts it into mechanical power. The power coefficient C_p is calculated by using the following formula [28]:

$$C_p(\lambda, \beta) = 0.22\left(\frac{116}{\beta} - 0.4 - 5\right)e^{-\frac{12.5}{\beta}}$$

with

$$\beta = \frac{1}{\frac{1}{\lambda + 0.08\lambda} - \frac{0.035}{\lambda^3 + 1}}.$$

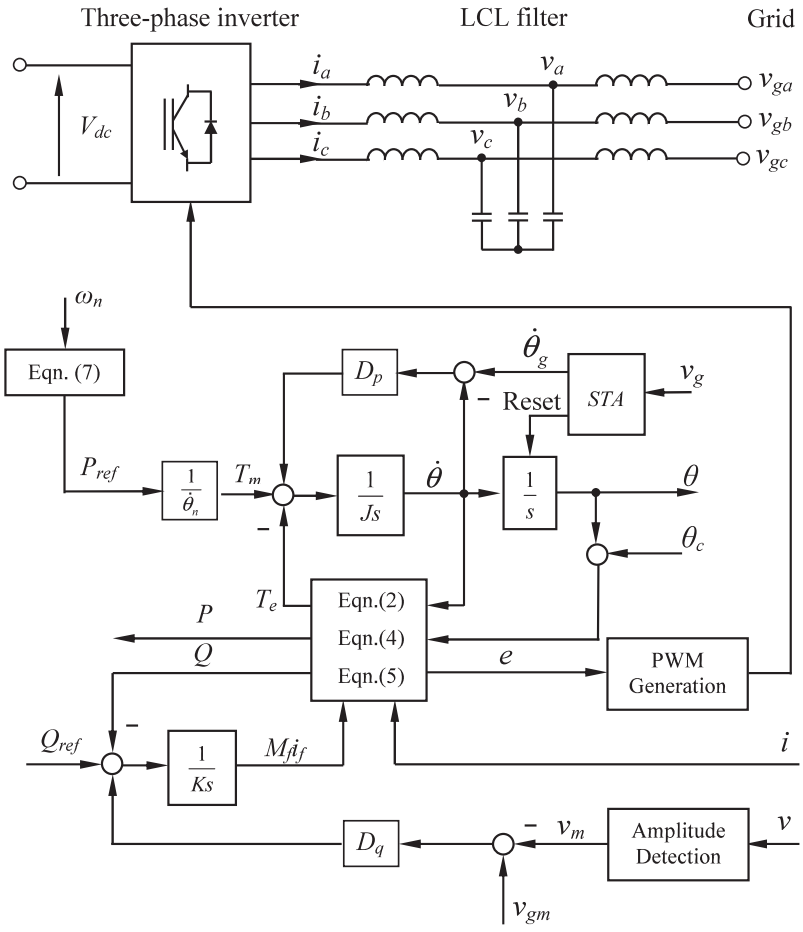

Fig. 5. Control structure for the grid-side converter.

Table 1
Parameters of the system.

Parameters	Value
Air density	1.2 (kg/m^3)
Rotor radius	1.2 (m)
Inertia of the PMSG	0.032 (kg m^2)
$M_f i_f$ of the PMSG	0.5 (V s)
Friction factor of the PMSG	0 (N m s)
Pole pairs of the PMSG	4
Winding inductance of the PMSG	4 (mH)
Winding resistance of the PMSG	0.135 (Ω)
DC-link voltage	400 (V)
DC-link capacitance	5000 (μF)
Inductance on the inverter side	1.1 (mH)
Inductance on the grid side	1.1 (mH)
Capacitance of the LCL filter	22 (μF)
Grid phase voltage (RMS)	110 (V)

Table 2
Control parameters for the rotor-side converter.

Parameters	Values	Parameters	Values
J_m	0.0122	K_p	0.8
D_{mp}	6.0793	K_i	2
K_m	2430.1		

For the simulated wind turbine, the optimal tip speed ratio λ_{opt} is 6.8 and the maximum power coefficient C_{pm} is 0.419.

5.1. Under the normal grid condition

The simulation was carried out according to the following sequence of actions:

(1) start the system, but keeping all the IGBTs off with the initial wind speed of 12 m/s to establish the DC link voltage first (with $R_{dc} = 150\ \Omega$);

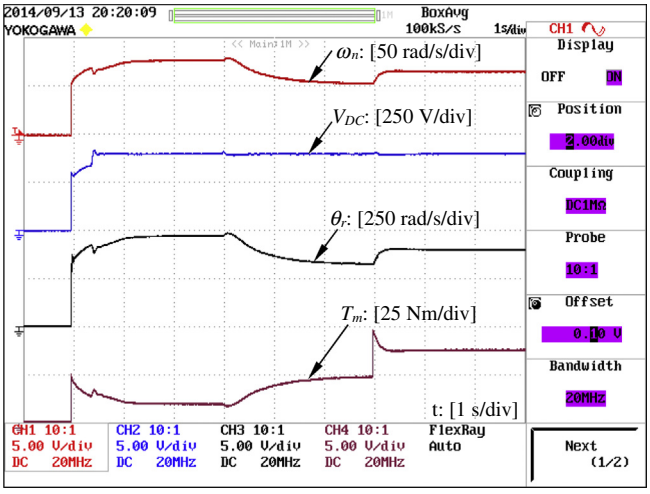

Fig. 6. Dynamic response of the rotor-side converter.

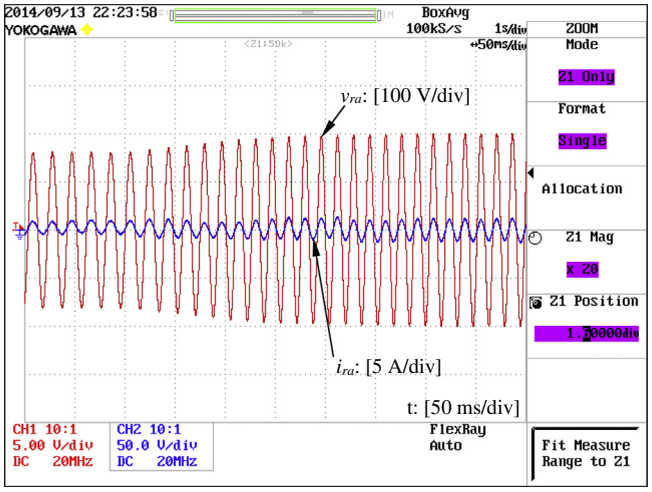

Fig. 7. Dynamic response of the rotor-side converter voltage and current during the wind change.

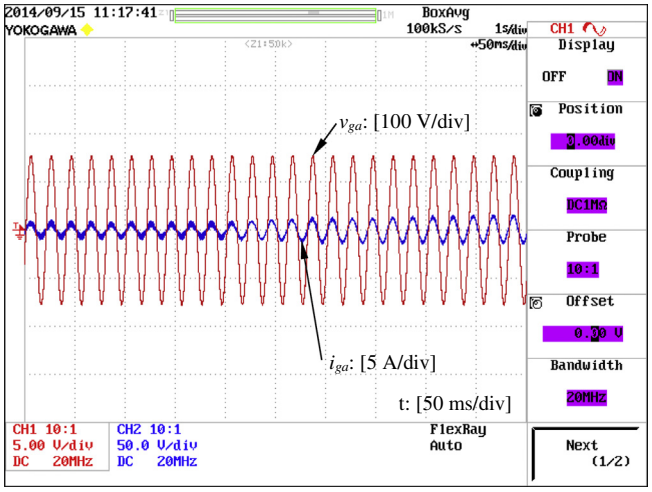

Fig. 9. Dynamic response of the rotor-side converter voltage and current during the wind change.

Table 3
Control parameters for the grid-side converter.

Parameters	Values	Parameters	Values
J	0.0122	K	2430.1
D_p	6.0793	D_q	386.7615

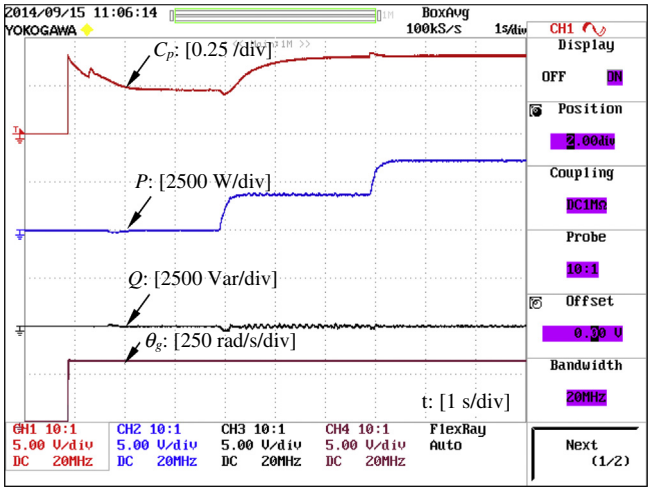

Fig. 8. Dynamic response of the grid-side converter.

(2) start operating the IGBTs for both converters at $t = 0.5$ s with $V_{ref} = 400$ V and $Q_{ref} = 0$ for the rotor-side converter to regulate the DC link voltage (with $R_{dc} = 150\,\Omega$) and with $P_{ref} = 0$ and $Q_{ref} = 0$ for the grid-side converter to synchronise with the grid;
(3) turn the circuit breaker on to connect the grid-side converter to the grid at $t = 0.8$ s;
(4) set $P_{ref} = 0.95K_{opt}\omega_n^3$ at $t = 3$ s and disconnect the DC load $R_{dc} = 150\,\Omega$ to send the maximum power to the grid;
(5) change the wind speed to 15 m/s at $t = 6$ s.

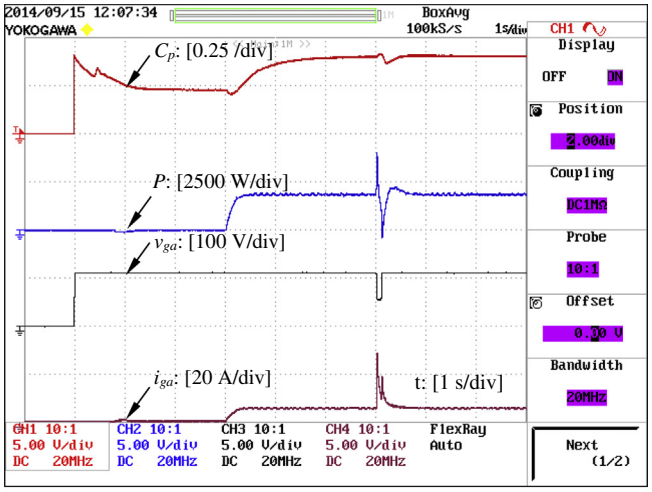

(a)

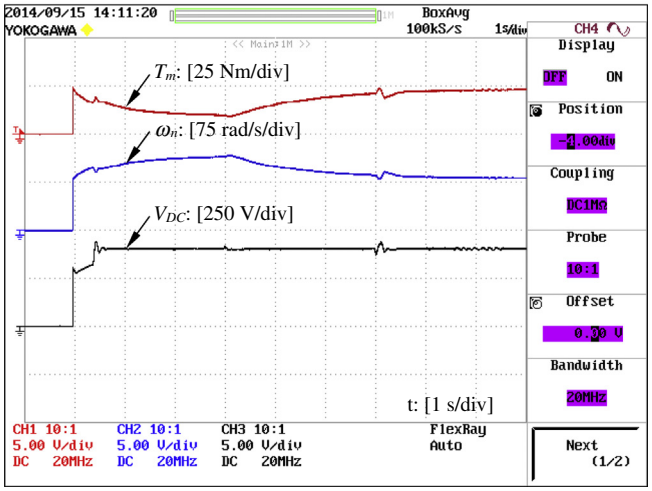

(b)

Fig. 10. Real time simulation results when the grid voltage drops by 50% at 6 s for 0.1 s.

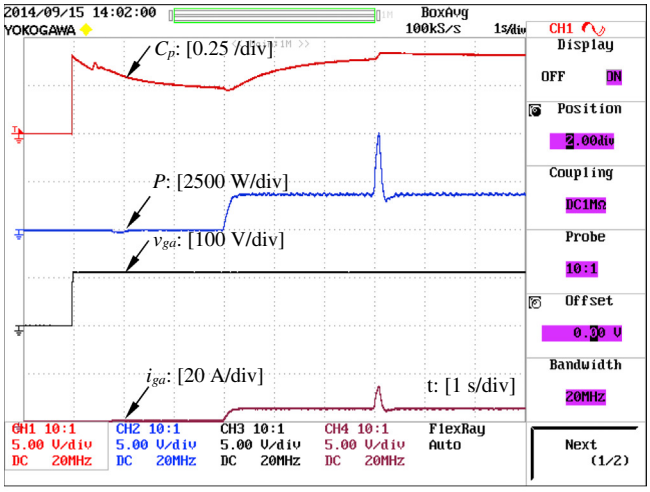

(a)

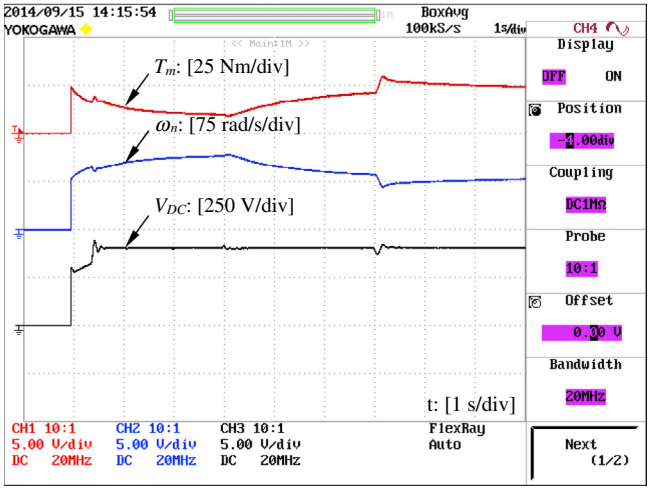

(b)

Fig. 11. Real time simulation results when the grid frequency drops by 1% at 6 s for 0.1 s.

It is worth noting that, in the real system, the DC load R_{dc} is often referred to as a DC link chopper, which can be activated when the DC link voltage exceeds a certain level. This level is chosen according to the converter ratings and is usually around 5% or 10% above the nominal DC link voltage [29].

5.1.1. Performance of the rotor-side converter

The parameters for the rotor-side converter are given in Table 2. The dynamic response of the rotor-side converter is shown in Fig. 6. It is observed that the DC-link voltage was maintained very well at 400 V after the system is connected to the grid. The rotor-side converter operated as a synchronverter was able to track the frequency of v_r, which is proportional to the rotor speed. During the wind change at $t = 6$ s, the responses of the rotor-side converter voltage and current are shown in Fig. 7, where the current drawn by the rotor-side converter is observed to be in phase with the voltage and, hence, the reactive power Q_m is zero, thus achieving the required unity power factor operation.

5.1.2. Performance of the grid-side converter

The parameters for the grid-side converter are shown in Table 3, which were chosen almost the same with the ones for the rotor-side converter. The real-time simulation results for the dynamic response are shown in Fig. 8. The connection of the system to the grid was very smooth without noticeable dynamics and the synchronverter frequency was able to track the grid frequency at all times. The power coefficient C_p was kept almost equal to its maximum value for the whole time after the system was requested to send the maximum power to the grid at $t = 3$ s and the real power P accurately tracked the reference power P_{ref}. Therefore, the maximum power point tracking was achieved by the grid-side converter, even after the wind speed changed at $t = 6$ s. The responses of the phase a of the grid current and the grid voltage are shown in Fig. 9, where it is clear that the unity power factor is achieved for the complete wind power system.

5.2. Under grid faults

In order to verify the fault ride-through capability of the proposed control strategy, two real-time simulations were carried out assuming 50% grid voltage drop and 1% grid frequency drop, respectively. Each fault occurred at 6 s and lasted for 0.1 s, respectively. The sequence of actions were the same as the ones in the previous experiments except that the fifth action was replaced with the grid faults at $t = 6$ s. The system parameters remained unchanged, apart from that the impedance of the feeder was considered explicitly as 2.2 mH and 0.2 Ω.

The system responses with the grid voltage dropped by 50% for 0.1 s are shown in Fig. 10. A peak was observed at the grid current when the grid voltage dropped, but it quickly settled down. The maximum current is about five times of the normal current. This is acceptable because inverters are often designed to be able to cope with excessive over-currents for a short period of time. Additionally, there is no noticeable change in the torque and the rotor speed, which means that the wind turbine and the PMSG worked properly during the grid voltage fault. The DC link voltage was controlled very well by the rotor-side converter and the maximum power coefficient was regulated to the desired value as well.

The system responses with the grid frequency dropped by 1% for 0.1 s are shown in Fig. 11. When the grid fault occurred, the output current increased immediately because of the small voltage drop on the inductor and when the fault was removed, the output current returned to the normal value very quickly. It is also worth mentioning that the output current was not excessively high. Moreover, the torque, rotor speed and the DC link voltage were all maintained around their values with very small overshoots.

6. Conclusions

In this paper, a synchronverter-based control strategy is proposed for back-to-back converters applied in variable speed wind turbines equipped with PMSG. The DC link voltage is controlled by the rotor-side converter and the MPPT is achieved by the grid-side converter. Both converters are controlled according to the recently-developed synchronverter technology. Hence, the whole system is equivalent to a generator–motor–generator system. Extended real-time simulation results verified that the proposed control strategy was able to maintain normal operation for the wind turbine with normal grid conditions and with grid faults, which improves the fault ride-through capability.

The method proposed in this paper presents an alternative strategy of controlling wind power systems with improved performance under both normal and grid fault conditions. A further investigation of the synchronverter operation with the dynamics of the complete wind power system will definitely strengthen and support the proposed approach. This provides an interesting topic for future research.

References

[1] Spera D. Wind turbine technology: fundamental concepts of wind turbine engineering. ASME Press; 2009.

[2] Ademi S, Jovanovic M. High-efficiency control of brushless doubly-fed machines for wind turbines and pump drives. Energy Convers Manage 2014;81(0):120–32.

[3] Mohammadi J, Afsharnia S, Vaez-Zadeh S. Efficient fault-ride-through control strategy of DFIG-based wind turbines during the grid faults. Energy Convers Manage 2014;78(0):88–95.

[4] Akel F, Ghennam T, Berkouk E, Laour M. An improved sensorless decoupled power control scheme of grid connected variable speed wind turbine generator. Energy Convers Manage 2014;78(0):584–94.

[5] Baroudi J, Dinavahi V, Knight A. A review of power converter topologies for wind generators. In: Proc. of IEEE international conference on electric machines and drives, 2005. p. 458–65.

[6] Seixas M, Melicio R, Mendes V. Fifth harmonic and sag impact on PMSG wind turbines with a balancing new strategy for capacitor voltages. Energy Convers Manage 2014;79(0):721–30.

[7] Masmoudi A, Krichen L, Ouali A. Voltage control of a variable speed wind turbine connected to an isolated load: experimental study. Energy Convers Manage 2012;59(0):19–26.

[8] Nasiri R, Radan A. Adaptive robust pole-placement control of 4-leg voltage-source inverters for standalone photovoltaic systems: considering digital delays. Energy Convers Manage 2011;52(2):1314–24.

[9] Hong C-M, Chen C-H, Tu C-S. Maximum power point tracking-based control algorithm for PMSG wind generation system without mechanical sensors. Energy Convers Manage 2013;69(0):58–67.

[10] Pena R, Clare J, Asher G. Doubly fed induction generator using back-to-back PWM converters and its application to variable-speed wind-energy generation. IEE Proc Electr Power Appl 1996;143(3):231–41.

[11] Pena R, Clare J, Asher G. A doubly fed induction generator using back-to-back PWM converters supplying an isolated load from a variable speed wind turbine. IEE Proc Electr Power Appl 1996;143(5):380–7.

[12] Cardenas R, Pena R. Sensorless vector control of induction machines for variable-speed wind energy applications. IEEE Trans Energy Convers 2004;19(1):196–205.

[13] Teodorescu R, Blaabjerg F. Flexible control of small wind turbines with grid failure detection operating in stand-alone and grid-connected mode. IEEE Trans Power Electron 2004;19(5):1323–32.

[14] Portillo R, Prats M, Leon J, Sanchez J, Carrasco J, Galvan E, et al. Modeling strategy for back-to-back three-level converters applied to high-power wind turbines. IEEE Trans Ind Electron 2006;53(5):1483–91.

[15] Bueno E, Cobreces S, Rodriguez F, Hernandez A, Espinosa F. Design of a back-to-back NPC converter interface for wind turbines with squirrel-cage induction generator. IEEE Trans Energy Convers 2008;23(3):932–45.

[16] Singh M, Khadkikar V, Chandra A. Grid synchronisation with harmonics and reactive power compensation capability of a permanent magnet synchronous generator-based variable speed wind energy conversion system. IET Proc Power Electron 2011;4(1):122–30.

[17] Konstantopoulos GC, Alexandridis AT. Full-scale modeling, control and analysis of grid-connected wind turbine induction generators with back-to-back AC/DC/AC converters, IEEE J Emerg Sel Top Power Electron, Early access. http://dx.doi.org/10.1109/JESTPE.2014.2325676.

[18] Gomis-Bellmunt O, Junyent-Ferre A, Sumper A, Bergas-Jan J. Ride-through control of a doubly fed induction generator under unbalanced voltage sags. IEEE Trans Energy Convers 2008;23(4):1036–45.

[19] McGranaghan M, Mueller D, Samotyj M. Voltage sags in industrial systems. IEEE Trans Ind Appl 1993;29(2):397–403.

[20] Bollen MH. Understanding power quality problems: voltage sags and interruptions. Wiley-IEEE Press; 2000.

[21] Yuan X, Wang F, Boroyevich D, Li Y, Burgos R. DC-link voltage control of a full power converter for wind generator operating in weak-grid systems. IEEE Trans Power Del 2009;24(9):2178–92.

[22] Hansen A, Michalke G. Multi-pole permanent magnet synchronous generator wind turbines' grid support capability in uninterrupted operation during grid faults. IET Proc Renew Power Gener 2009;3(3):333–48.

[23] Kim K-H, Jeung Y-C, Lee D-C, Kim H-G. Robust control of PMSG wind turbine systems with back-to-back PWM converters. In: Proc. of the 2nd power electronics for distributed generation systems (PEDG); 2010. p. 433–7.

[24] Bose B. Modern power electronics and AC drives. Prentice-Hall (NJ): Englewood Cliffs; 2001.

[25] Zhong Q-C, Weiss G. Synchronverters: inverters that mimic synchronous generators. IEEE Trans Ind Electron 2011;58(4):1259–67.

[26] Ziarani AK, Konrad A, Sinclair AN. A novel time-domain method of analysis of pulsed sine wave signals. IEEE Trans Instrum Meas 2003;52(3):809–14.

[27] Ziarani AK, Konrad A. A method of extraction of nonstationary sinusoids. Signal Process 2004;84(8):1323–46.

[28] Sun T, Chen Z, Blaabjerg F, Voltage recovery of grid-connected wind turbines after a short-circuit fault. In: Proc. of industrial electronics society (IECON); 2003. p. 2723–8.

[29] Chaudhary SK, Teodorescu R, Rodriguez P, Kjar PC. Chopper controlled resistors in VSC-HVDC transmission for WPP with full-scale converters. In: 2009 IEEE PES/IAS conference on sustainable alternative energy (SAE), Valencia, Spain; 2009. p. 1–8.